

VEHICLE SIMULATION RESULTS FOR PLUG-IN HEV BATTERY REQUIREMENTS

October 1, 2006

Phillip Sharer
Argonne National Laboratory

Aymeric Rousseau, Paul Nelson, Sylvain Pagerit
Argonne National Laboratory

Abstract

Plug-in Hybrid Electric Vehicles (PHEVs) have the ability to drastically reduce petroleum use. The FreedomCAR Office of Vehicle Technology is developing a program to study the potential of the technology. The first step in the program is to define the requirements of PHEV components. As the battery appears to be the main technical barrier, both from a performance and cost perspective, the main efforts have been focused on that component. Working with FreedomCAR energy storage and vehicle experts, Argonne National Laboratory (Argonne) researchers have developed a process to define the requirements of energy storage systems for plug-in applications. This paper describes the impact of All Electric Range (AER), drive cycle, and control strategy on battery requirements.

Keywords: Plug-in Hybrid, Hybrid Strategy, Modeling, Simulation, Energy Efficiency.

1 Introduction

Relatively detailed comparisons between plug-in hybrid powertrains and hybrid powertrains were recently completed [1] However, these studies did not examine the potential benefit of using a Li-ion battery. To evaluate the battery requirements for different PHEV options, Argonne's vehicle simulation tool, Powertrain System Analysis Toolkit (PSAT), was used with a battery model designed by Argonne's battery research group.

PSAT [2, 3], developed with MATLAB and Simulink, is a vehicle-modeling package used to estimate performance and fuel economy. In PSAT, a driver model estimates the wheel torque that the vehicle needs to follow a predetermined speed trace. Using the driver model's estimate of wheel torque, the vehicle controller calculates a command for each component in the powertrain, such as throttle position for the engine, displacement for the clutch, gear number for the transmission, or mechanical braking for the wheels. Since components in PSAT are commanded, real control strategies can be used along with advanced component models, which account for transient effects (e.g., engine starting, clutch engagement/disengagement, or shifting). Finally, by using test data measured at Argonne's Advanced Powertrain Research Facility, PSAT has been shown to predict the fuel economy of several hybrid vehicles within 5% on the combined cycle. PSAT is the primary vehicle simulation package used to support the U.S. Department of Energy (DOE) FreedomCAR R&D activities.

In this study, we describe the component models and control strategies developed to characterize Plug-in Hybrid Electric Vehicles (PHEVs). The impact of All Electric Range (AER) on fuel efficiency will be analyzed to provide direction on the most appropriate sizing strategy. Then, the main battery parameters, including energy, power, current and voltage, will be evaluated. Finally, we will study the uncertainty in the requirements due to vehicle class, driving cycle, and control strategy settings.

2 Modeling Assumptions

2.1 Vehicle

Table 1 shows the characteristics of the midsize car that were used in simulation. The engine, electric machine, and battery were sized to achieve the required performance criteria shown in Table 2. The engine and the electric machine were sized on the basis of power, while the battery was sized on the basis of both power and energy. The battery model and sizing algorithm are described in greater detail later in the paper.

Table 1: Main Specifications of the Vehicle

Component	Specifications
Engine	Gasoline based on LK5 data
Electric machine	UQM SR218N
Battery	Li-ion – VL41M
Transmission	5-speed manual transmission Ratio: [3.42, 2.14, 1.45, 1.03, 0.77]
Frontal Area	2.244 m ²
Final Drive Ratio	3.8
Drag Coefficient	0.315
Rolling Resist.	0.008 (plus speed-related term)
Wheel radius	0.3175 m

Table 2: Performance Requirements

Parameter	Unit	Value
0–60mph	s	9 +/- 0.1
0–30mph	s	3
Grade at 55 mph	%	6
Maximum Speed	mph	> 100

As shown in Figure 1, the configuration selected is a pre-transmission parallel hybrid, similar to the one used in the DaimlerChrysler Sprinter Van [1].

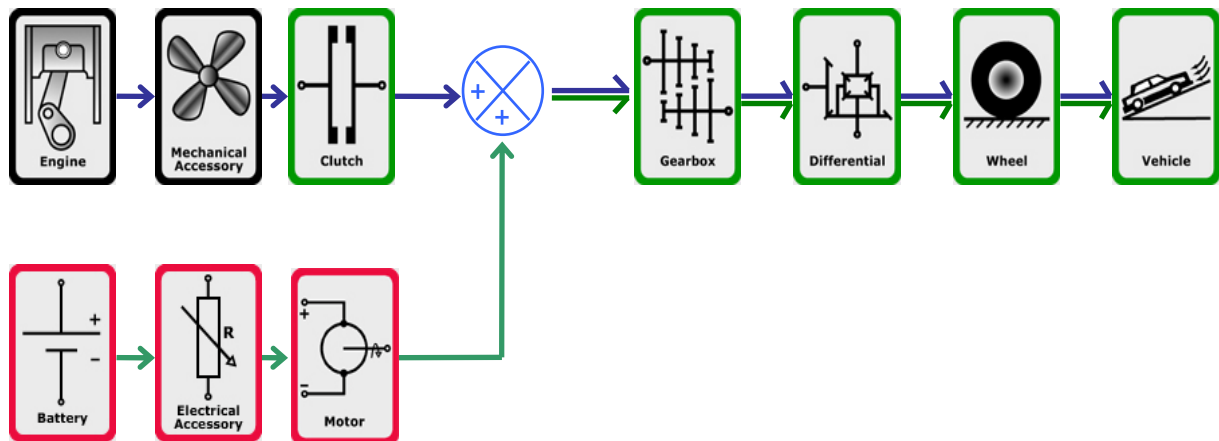


Figure 1: Configuration Selected – Pre-Transmission Parallel HEV

To account for uncertainties associated with component technology, both slow and fast technology growth cases were considered. Fast technology growth represents the consequences of achieving the FreedomCAR goals, while slow technology growth represents the consequences of more conservative improvements.

2.2 Battery

In this study, equations were derived for calculating the impedance of a plug-in hybrid vehicle battery for use in simulating the battery behavior under driving conditions. Developing the equations for expressing battery resistance for a plug-in hybrid vehicle battery is more complex than developing those for a standard hybrid vehicle because the plug-in battery may be charged and discharged during vehicle operation for periods lasting several minutes. Ideally, the equations should be able to reproduce the measured voltage curves for a complete discharge and charge at constant current, as well as the battery resistance under conditions of rapidly changing currents. Current and voltage data taken at Argonne National Laboratory were available for a cell fabricated by SAFT, Inc., which is somewhat similar to its 41-Ah lithium-ion cell (designated VL 41M listed on SAFT's web site). The VL41M cell has a capacity of 41-Ah at the 3-h rate and a power of 1,000 W (400 A at 2.5V) at 80% Depth of Discharge (DOD). The data for the cell measured at Argonne were for a 3-h discharge at constant current and for Hybrid Pulse Power Characterization (HPPC) tests. These data were fit to an electronic simulation model with two time constants (Fig. 2) of the form:

$$(OCV - V_L)/I_L = R = R_o + R_{p1} * I_{p1}/I_L + R_{p2} * I_{p2}/I_L$$

In this relationship, OCV and V_L are the open circuit and load voltages; R , R_o , R_{p1} , and R_{p2} , are the total battery impedance, the ohmic resistance, and the polarization impedances; and I_{p1}/I_L and I_{p2}/I_L are the ratios of the polarization currents to the load current. The polarization currents are determined by integration of the equation $dI_p/dt = (I_L - I_p)/\tau$ for each of the polarization impedances (where τ_1 and τ_2 are time constants of 22.8 and 270 s, respectively), as in an earlier study that also used two polarization impedances [4] and in the PNGV Lumped Parameter Model [5] of the United States Department of Energy, which was a similar model with one polarization impedance. The parameters in the equation (OCV , R_o , R_{p1} , R_{p2}) were selected to match the measured data for both the 3-h discharge and the HPPC data for the entire range of the discharge, and these parameters were presented in the form of a lookup table with values from 0% to 100% state of charge at 10% intervals (τ_1 and τ_2 were held constant over the entire discharge). These results were converted to a similar table for the SAFT 41-Ah cell, VL41M, by use of a multiplying factor that matched the calculated impedance at 80% DOD with that given for the VL41M cell.

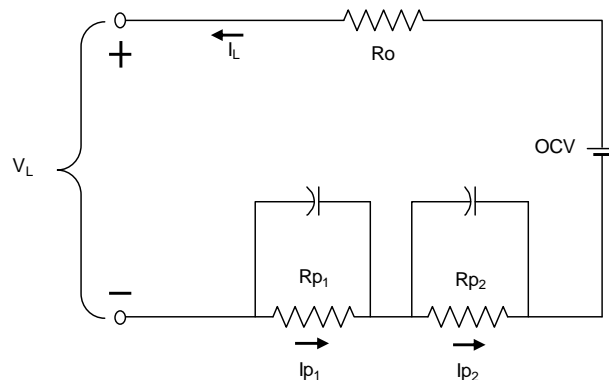


Figure 2: Battery Electric Circuit Model

The utility of the model was further extended to include cells of the same chemistry, but with capacities in the range of 10–100 Ah and capacity-to-power ratios (C/P) of 0.75–3.0 times that of the VL41M cell and for batteries containing any number of such cells. This was done by developing a set of equations used to determine the multiplying factor for converting the lookup table developed for the

parameters of the VL41M cell to the appropriate values for the desired cell capacity and power. For instance, some of the equations (with compatible dimensions) are shown here:

$(C/P)_{41}$ = ratio of capacity to power at 80% DOD and 2.5 V for VL41M cell

C_C = capacity of simulated battery cell

F_C = capacity factor for cell = $(C/P)_C / (C/P)_{41}$

M = number of 6-cell modules in battery

N = number of cells in battery = $6 \times M$

R_{41} = resistance of VL41 M cell = $R_o + R_{p1} \times I_{p1}/I_L + R_{p2} \times I_{p2}/I_L$

R_B = resistance of battery = $R_{41} \times F_C \times (41/C_C) \times N$

P_B = power of battery at = $P_{41}/F_C \times C_C/41 \times N$

The model so derived makes it possible to simulate battery behavior for batteries suited to PHEVs with electric ranges of 20–60 miles.

2.3 Component Sizing Process

To quickly size the component models of the powertrain, an automated sizing process was developed. A flow chart illustrating the logic of the sizing algorithm is shown in Figure 3. While engine power is the only variable for conventional vehicles, HEVs have two variables with the additional electric machine power. PHEVs add yet another degree of freedom with the battery energy. On the basis of assumptions about the vehicle, the peak electric machine mechanical power is defined as the peak power required for the vehicle to follow the Urban Driving Dynamometer Schedule (UDDS) driving cycle. The battery peak discharge power is then defined as the electrical power that the motor requires to produce the peak mechanical power needed for the vehicle to follow the UDDS cycle. The engine is then sized to achieve the gradeability requirement of the vehicle.

The 0–60 performance requirement for the vehicle is satisfied implicitly by the constraints on the peak motor power and the peak engine power. The power required under the conditions of the UDDS cycle with only the motor running and the vehicle driving up a 6% grade with just the engine at 55 mph exceeds the power requirement imposed on these components based on the need to achieve the desired performance.

Finally, the battery energy is sized to achieve the required AER of the vehicle. The AER is defined as the distance the vehicle can travel without starting the engine. It is important to notice that a separate control algorithm is used to simulate the AER. This controller forces the engine to remain off throughout the cycle, regardless of the torque request from the driver. As during the previous stages, the component masses have changes, and so one needs to verify that the difference between the original mass (for which the components have been sized) is close to the final mass (modified after sizing). If this is not the case, the process will perform another iteration. Once the convergence is achieved, the battery is oversized to take into account battery aging. The battery power is oversized by 30% and its energy by 20%. This assumption will be revisited once more battery data become available.

Seven AER values (7.5, 10, 20, 30, 40, 50, and 60 mi) were simulated. The battery characteristics for each vehicle are provided in Appendix 1. Figure 4 shows three ranges that were defined for each vehicle. The end-of-life (EOL) AER confirms the validity of the sizing algorithm. One notices that an additional AER is available at the beginning of life (BOL).

Excess energy is added to maintain a consistent range throughout the life of the vehicle. At the beginning of life, the control strategy would limit the vehicle range to the value it has at the end of its life, and the additional energy of the battery would not be used. As the battery ages, it loses this excess energy until at the EOL it has enough energy just to meet the range requirement. Thus, the user of the vehicle would never experience a gradual loss in vehicle AER.

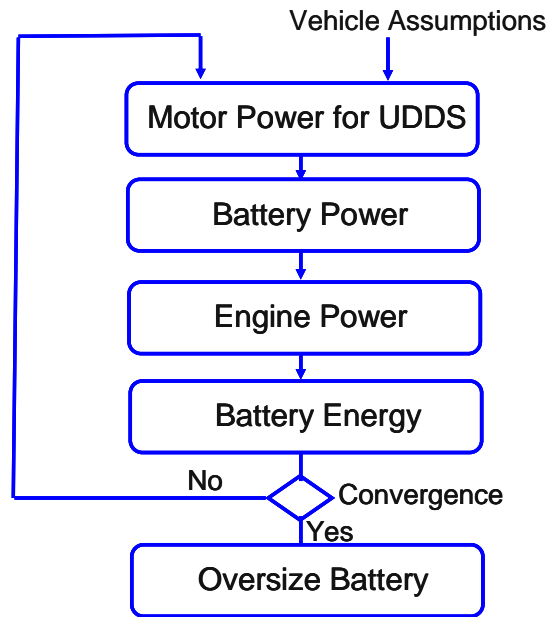


Figure 3: Vehicle Component Sizing Process

Finally, during the cycle, according to the request of the driver model, the engine is turned on, which expends fuel but conserves battery energy so that more miles can be traveled before the battery reaches its discharged state. The operating mode that turns the engine on while still depleting the battery is called the Charge Depleting (CD) mode. The additional distance traveled during CD mode depends on the control strategy, which is described in the following section.

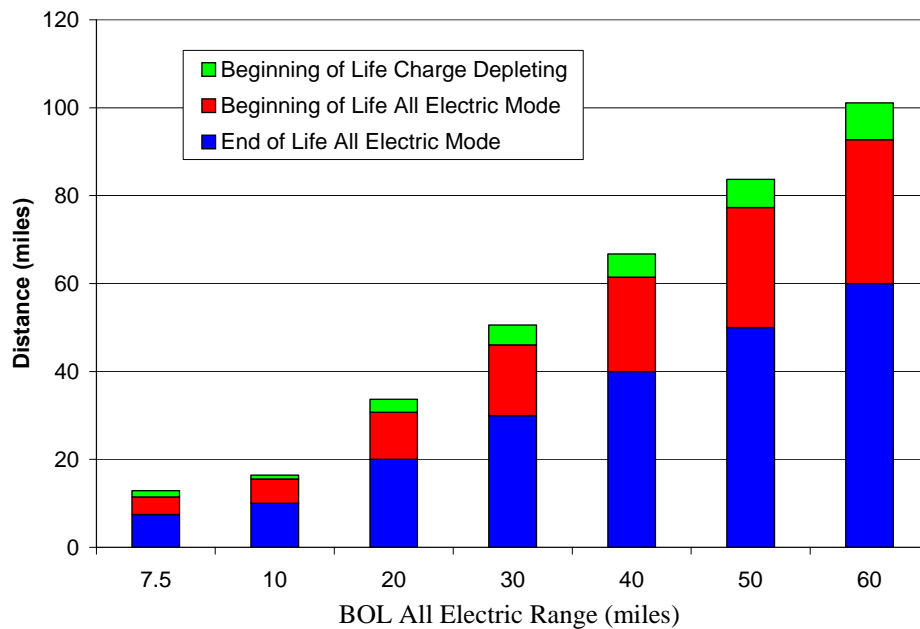


Figure 4: Results of Vehicle Component Sizing Process

2.4 Control Strategy

The control strategy can be separated into two distinct modes, as shown in Figure 5:

- CD, in which the electric energy is used as the primary mover, and
- Charge-sustaining (CS), which is similar to that in current HEVs.

Initial state-of-charge (SOC) of the battery, which is also the battery’s maximum charge, is 90%, and the final SOC of the battery, which is also the battery’s minimum charge, is 30%. For the CD mode, the engine logic was written in StateFlow and used several conditions, such as battery SOC, motor power limits, and vehicle speed, to determine when the engine should turn on and the output torque of the engine. The logic of the CS mode was similar to that of current HEVs.

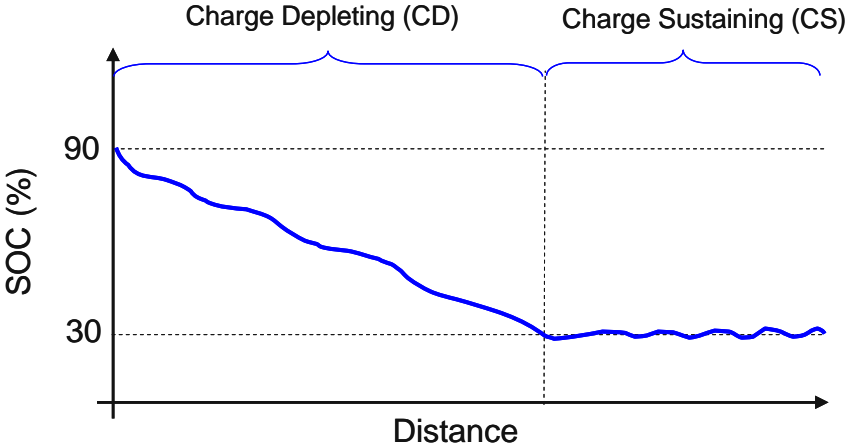


Figure 5: Control Strategy Schematic

3 Vehicle Level Results

Figure 6 shows the energy consumption in units of watt-hour per mile for both the battery and the engine for the different CD ranges considered. Note that both consumptions increase with the CD range as a result of an increase in vehicle mass. However, the increase is not significant (310–340 Wh/mi) for the battery and will only have a small impact on the requirements.

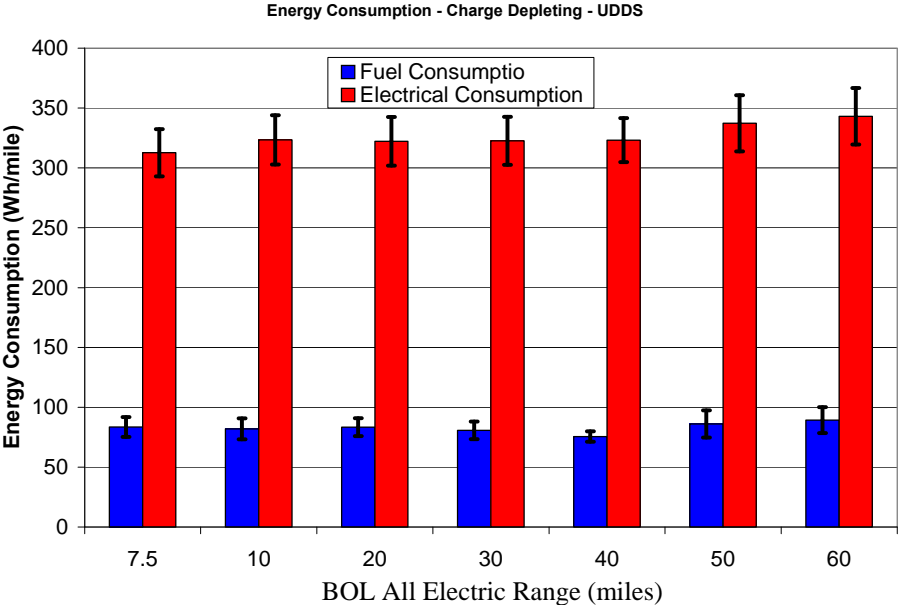


Figure 6: Charge-Depleting Consumption

When looking at energy consumption during the CS operating mode of each vehicle, which is shown in Figure 7, note the same trend of a small increase in the energy consumption with increased CD range.

Thus, increased CD range can be attained without significantly reducing the efficiency of the vehicle during CS operation. This is attributed to the high specific energy of the Li-ion battery. More energy storage can be added without a major mass penalty.

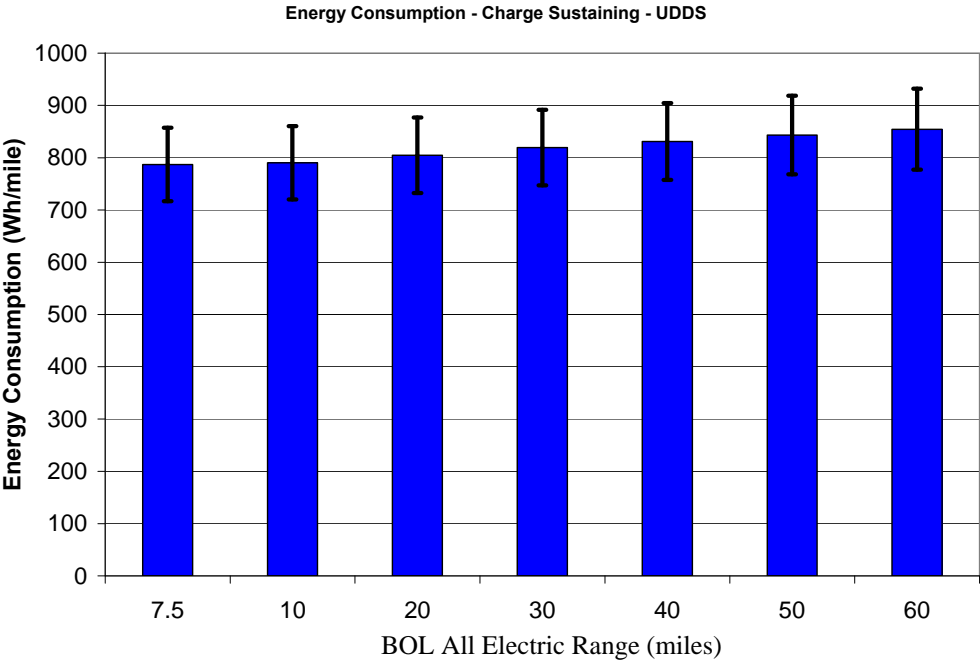


Figure 7: Charge-Sustaining Consumption

4 Battery Parameters

4.1 Energy

The energy needed to satisfy the all-electric-range requirement drives the battery requirements for PHEVs. As can be seen in Figure 8, the required usable energy is a linear function of the AER. A critical issue related to sizing the battery is to determine its minimum state of charge (SOC). As the minimum SOC of the battery is lowered more energy can be extracted from the battery which allows the vehicle to go the same distance with fewer battery cells; however, a lower minimum SOC also shortens the life of the battery. The vehicle designer chooses between battery size and battery life in their design

In our study, to preserve the life of the battery, the maximum SOC was set to 90% and the minimum SOC was set to 30%— thus, the control strategy uses 60% of the total energy stored in the battery to propel the vehicle.

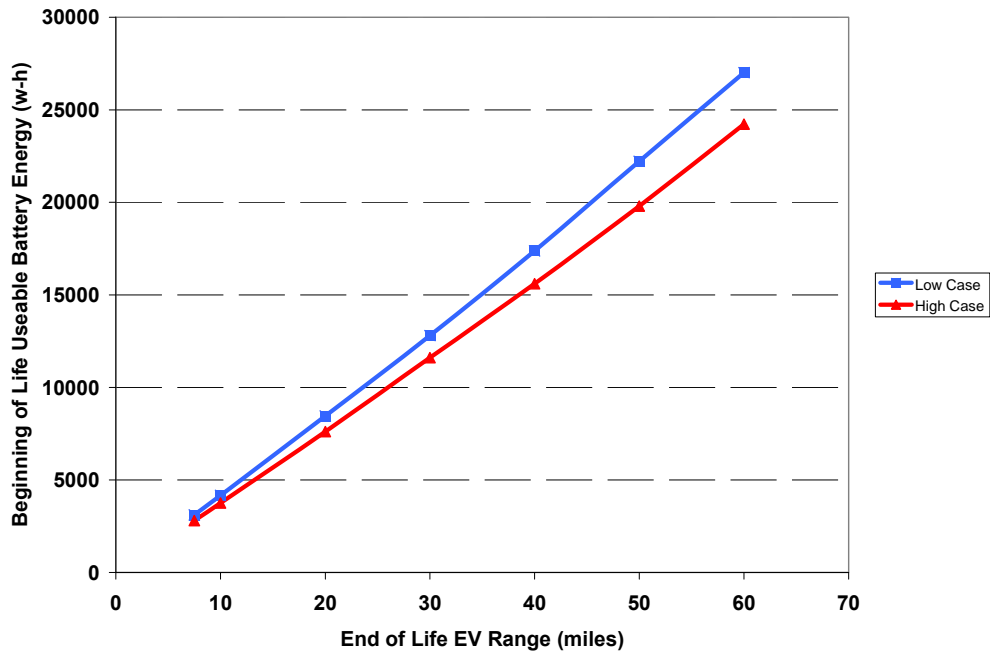


Figure 8: Usable Energy as a Function of All-Electric Range

4.2 Power

Because vehicle mass is relatively insensitive to AER increases (250 kg from 7.5 to 60 mi AER), the power of each component remains nearly constant as AER increases. Figure 9 shows the peak electric machine power required to follow the UDSS driving cycle.

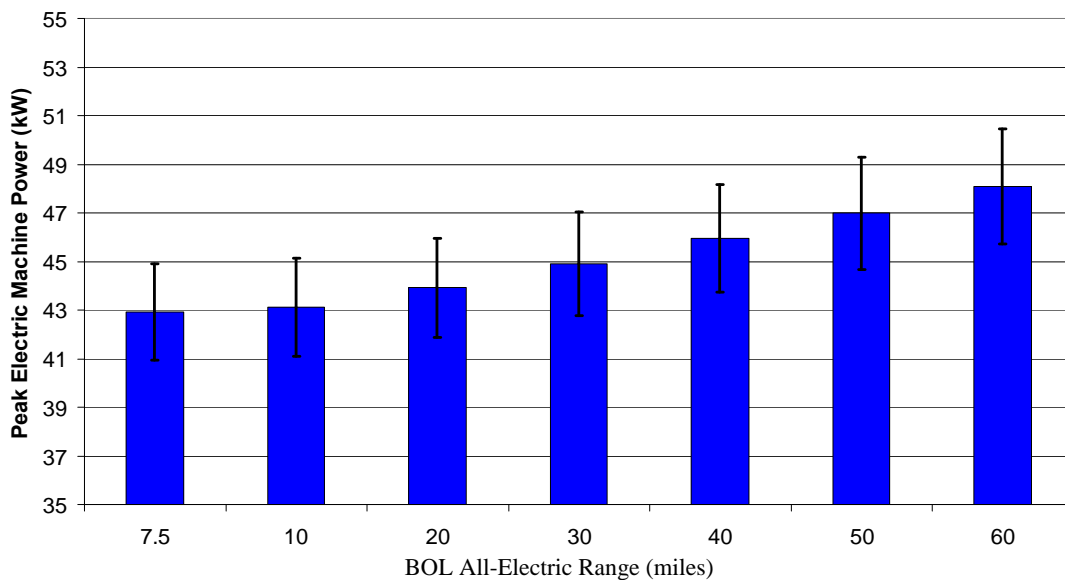


Figure 9: Peak Electric Machine Power as a Function of All-Electric Range

The constant power characteristic combined with a linear increase in usable energy leads to the Power-to-Energy (P/E) ratio characteristics shown in Figure 10. Note that the P/E ratio decreases with increased AER. This demonstrates the need to have a separate battery design for each range.

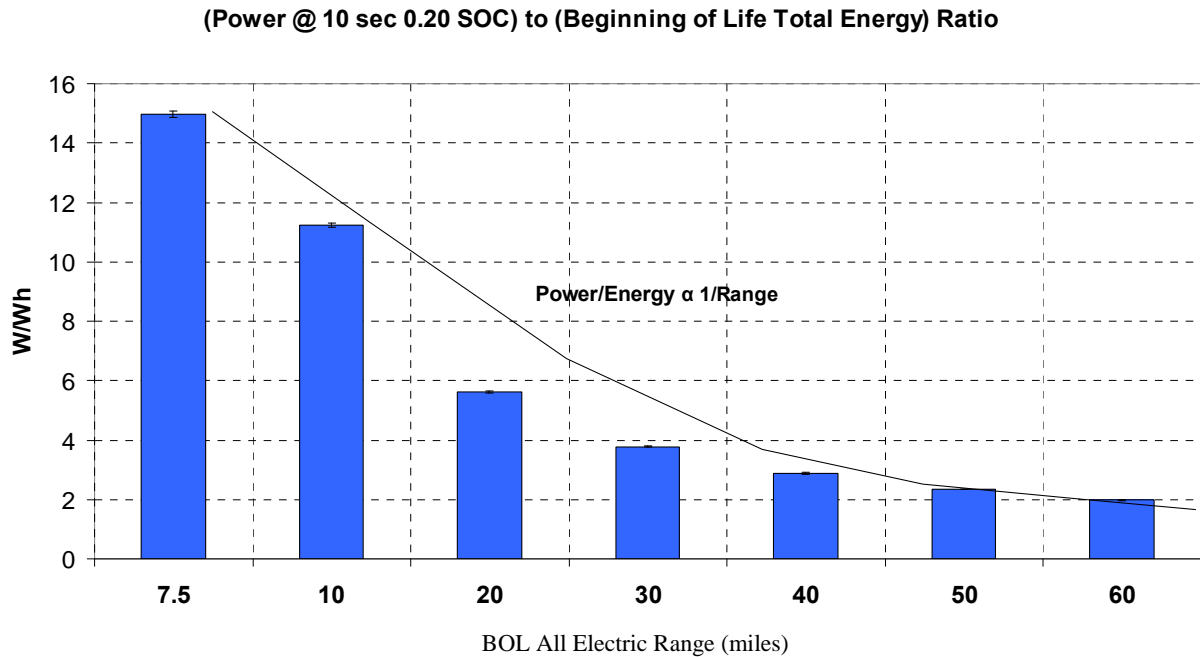


Figure 10: Power-to-Energy Ratio Requirements as a Function of All-Electric Range

The power requirement for a battery is specified not as a constant but rather as a pulse. Thus, not only is the magnitude of the pulse given, but also its duration. Figure 11 was specifically developed to address this need.

After the simulation, the PSAT post-processing routine examines every charging pulse that occurred during the cycle. Each pulse is divided by time into seconds, and the data for the first second of every pulse is statistically analyzed. Then, the data for the next second is analyzed and so on. From these data, a charging profile can be assembled by plotting the average charging power of each second versus time. The maximum and minimum values can also be plotted. This process gives an average charging pulse for the cycle. By understanding this average pulse behavior in greater detail, it might be possible to craft less-stringent battery requirements that allow a faster introduction of the technology in the market place. For example, instead of stating that a maximum charging power of 20 kW needs to be sustained for 13 s, one can use Figure 11 to argue that the system only requires 20 kW of charging power for 3 s, 15 kW for 10 s, and 0 kW after 13 s. Figure 11 also demonstrates that the AER does not significantly impact the component power requirements.

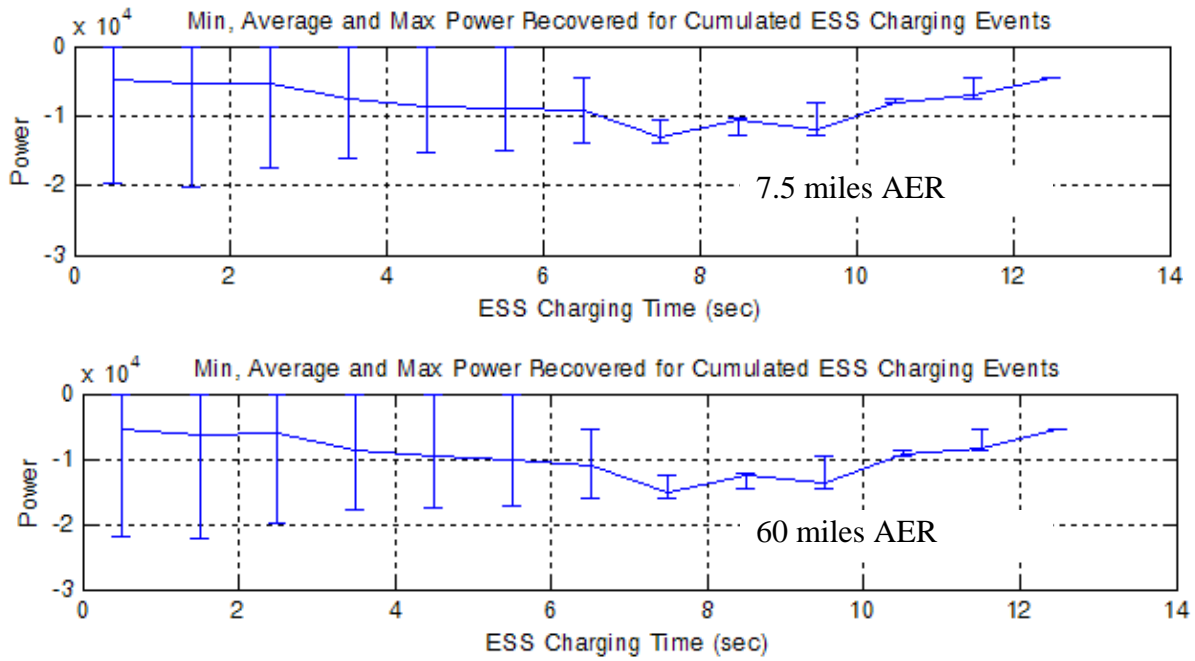


Figure 11: Impact of AER on Regenerative Power Requirements – UDDS Cycle

4.3 Current

Figure 12 shows the distribution of the current during charging events for the US06 drive cycle. Most of the events occur at less than 80 A, with a maximum of 120 A. These values are not problematic because current batteries are able to sustain far greater current. For example, the JCS VL41M can handle 400 A for 10 s and 150 A continuously.

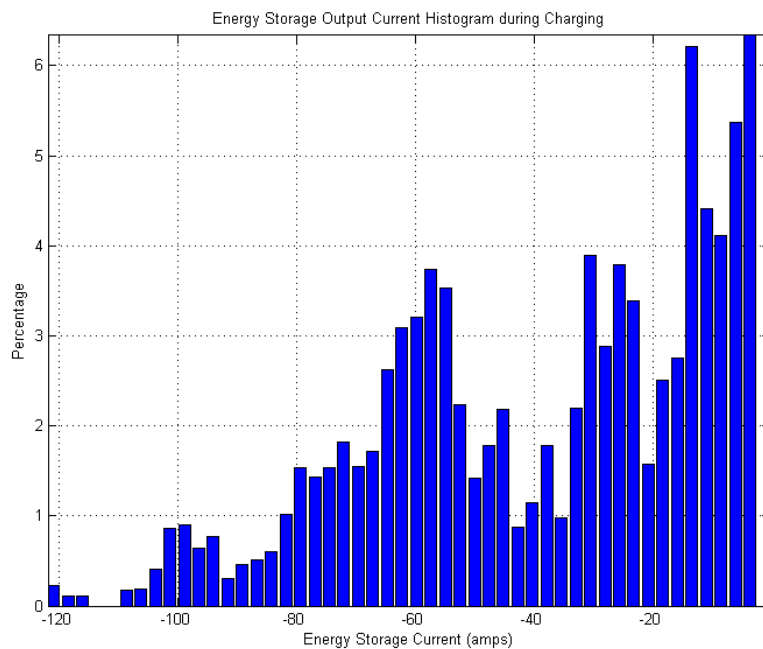


Figure 12: Battery Current Distribution – US06 Cycle – 40 miles AER

4.4 Voltage

As previously discussed, energy is the key parameter for sizing the battery. Once the usable energy is defined, one more degree of freedom remains between the battery pack voltage and its capacity. We decided to maintain the pack voltage between 200 and 300 V on the basis of current technologies (Figure 13). As a consequence, the capacity will increase with the AER until the limit of 90 Ah is reached at 30 miles AER. Increased AER values (40–60 mi) will then lead to increased battery voltage, which might be problematic on the vehicle side. An option would be to use higher capacity, but this would lead to other issues, such as safety.

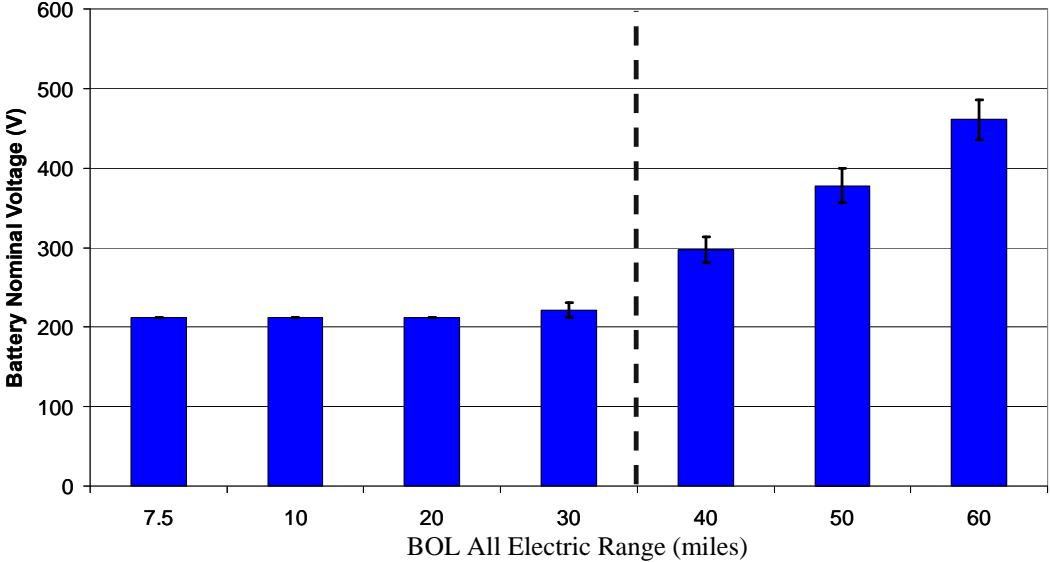


Figure 13: Battery Pack Voltage as a function of AER

5 Uncertainty Evaluation

5.1 Impact of Component Sizing

One of the key assumptions of the sizing process was that the electric motor was sized to follow the UDDS driving cycle. Figure 14 shows the impact of using twice the electric machine power. Note that the distribution is very similar. In the case of the larger motor, the peak current is higher (190 vs. 120 A). However, these higher currents rarely occur and are still well below the maximum capabilities of existing battery technologies.

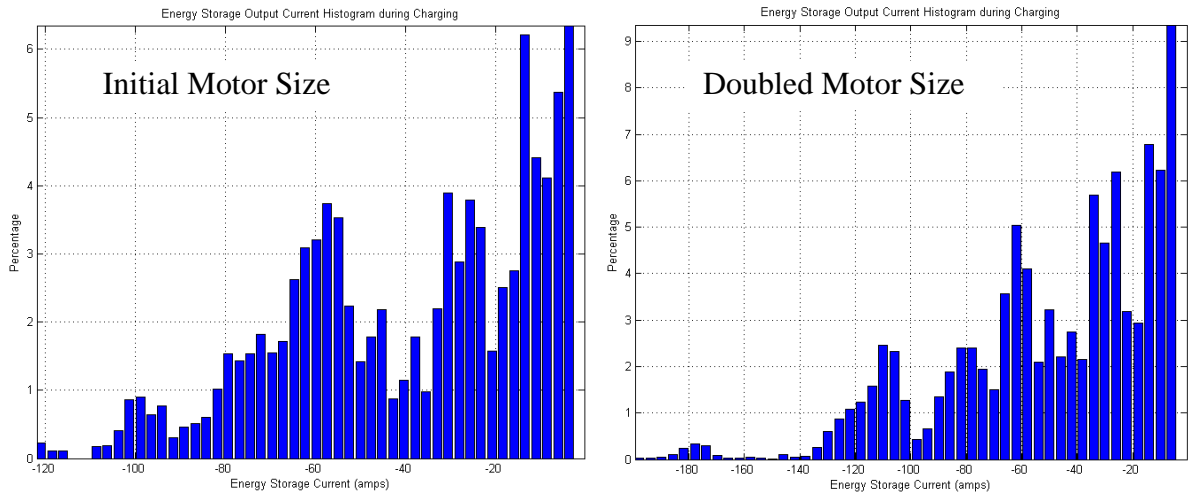


Figure 14: Battery Current Distribution Change with Different Sizes of Motor (US06 -40 mi AER)

5.2 Impact of SOC Operating Range

The other key parameter affecting the battery size is the difference between maximum SOC and minimum SOC. This difference can be referred to as the SOC window. The SOC window defines the relationship between the battery's total energy and its usable energy. Two options have been considered: with and without battery resizing.

5.2.1 Without Battery Resizing

When the SOC window is changed but the battery is unchanged, the useable energy increases and the range will increase. Figure 15 shows that the engine energy is not modified by the change in delta SOC value. In other words, the engine is not more or less efficient because of the SOC window.

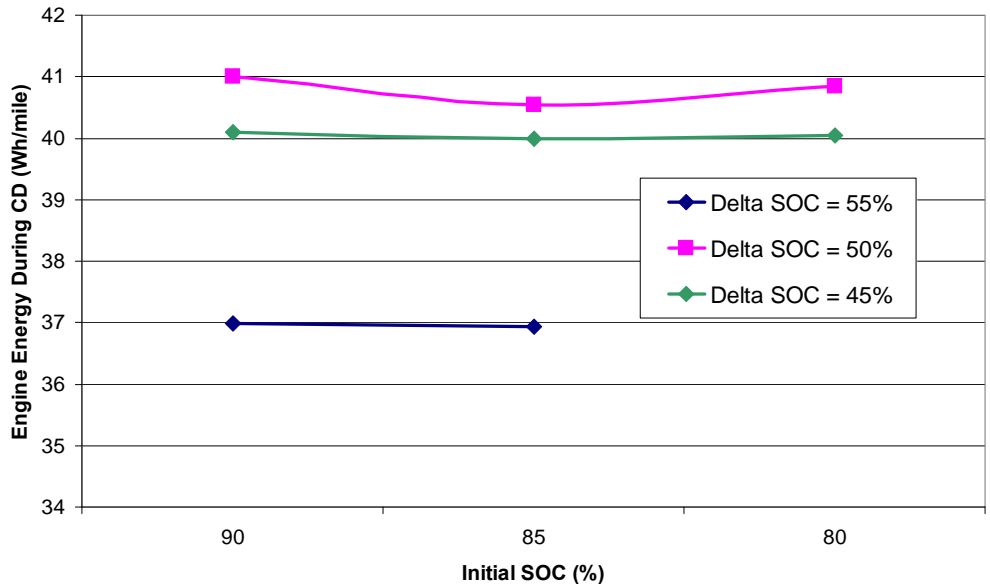


Figure 15: Engine Consumption with Different SOC Window – No Battery Resizing

5.2.2 With Battery Resizing

A more thorough approach would consist of resizing the battery to maintain the desired AER as the SOC window is modified. Figure 16 shows the engine fuel consumed for the same AER with different

sizes of battery. As mentioned previously, there is a very small difference in energy consumption by the engine. A trade-off has to be taken into account as a decrease in SOC range leads to longer life while increases cost as a result of a larger number of cells. Further analysis on the life cycle will be performed when additional test data are available.

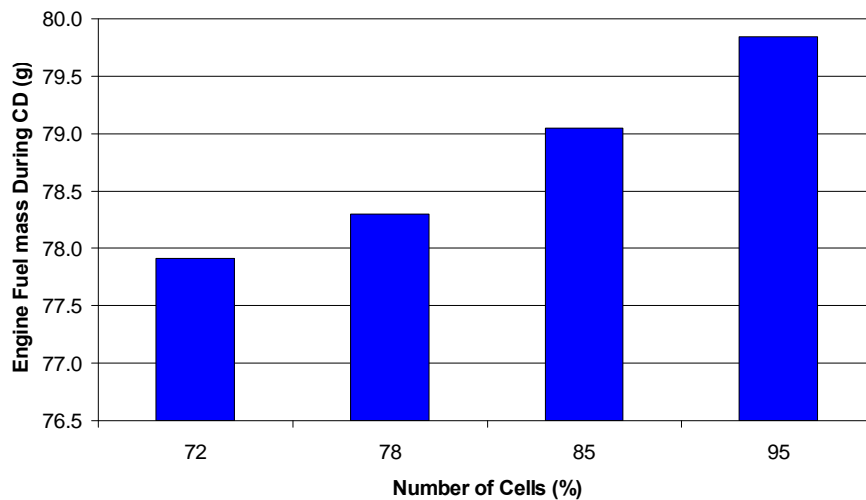


Figure 16: Engine Consumption with Different SOC Window – With Battery Resizing

6 Conclusions and Future Work

Component models and control strategies have been developed and implemented in PSAT to study the impact of AER, drive cycle, control strategy, and component sizing on the battery requirements. The following conclusions can be stated:

- The battery energy is approximately a linear function of AER.
- AER is not a valid parameter to define the requirements because it depends on numerous parameters, including vehicle class, drive cycle, and control strategy, among others.
- Power requirements are not influenced by the AER as a result of the high specific energy of the Li-Ion battery.
- The high specific power of Li-ion technologies does not have a significant influence on vehicle mass. Specific energy has the greatest affect on vehicle mass.
- Battery pack voltage needs to be taken into consideration for high AER (above 40 mi).

Future work will involve undertaking a similar study on the midsize SUV platform using existing state-of-the-art battery packs that will be tested and characterized. Information will then be provided to the FreedomCAR Energy Storage Tech Team to define the final requirements.

References

- [1] Graham, B., “*Plug-in Hybrid Electric Vehicle, A Market Transformation Challenge: the DaimlerChrysler/EPRI Sprinter Van PHEV Program*,” EVS21, April 2005.
- [2] Argonne National Laboratory, PSAT (Powertrain Systems Analysis Toolkit), <http://www.transportation.anl.gov/>.
- [3] Rousseau, A.; Sharer, P.; and Besnier, F., “*Feasibility of Reusable Vehicle Modeling: Application to Hybrid Vehicles*,” SAE paper 2004-01-1618, SAE World Congress, Detroit, March 2004, <http://www.eere.energy.gov/vehiclesandfuels>.
- [4] Nelson, P., “*Modeling the Performance of Lithium-Ion Batteries for Fuel Cell Vehicles*,” SAE paper 2003-01-2285 in SP-1789, Costa Mesa, CA, June 23–25, 2003.

[5] *PNGV Battery Test Manual*, revision 3, DOE/ID-10597, U.S. Department of Energy, 2001.

Authors



Phillip Sharer, Research Engineer, Argonne National Laboratory, 9700 South Cass Avenue, Argonne, IL 60439-4815, USA, psharer@anl.gov

Phillip Sharer is Systems Analysis Engineer at Argonne National Laboratory. He received a Master of Science in Engineering from Purdue University Calumet in 2002. He has over five years of experience modeling hybrid electric vehicles using PSAT at Argonne.



Aymeric Rousseau, Research Engineer, Argonne National Laboratory, 9700 South Cass Avenue, Argonne, IL 60439-4815, USA, arouseau@anl.gov

Aymeric Rousseau is head of the Advanced Powertrain Vehicles Modeling Department at Argonne National Laboratory. He received his engineering diploma at the Industrial System Engineering School in La Rochelle, France, in 1997.



Sylvain Pagerit, Research Engineer, Argonne National Laboratory, 9700 South Cass Avenue, Argonne, IL 60439-4815, USA, spagerit@anl.gov

Sylvain Pagerit received a Master of Science in Industrial Engineering from the Ecole des Mines de Nantes, France, in 2000, as well as a Master of Science in Electrical Engineering from the Georgia Institute of Technology, Atlanta, in 2001.



Paul Nelson, Senior Chemical Engineer, Argonne National Laboratory, 9700 South Cass Avenue, Argonne, IL 60439-4815, USA, nelson@cmt.anl.gov

Paul Nelson received his Ph.D. in Chemical Engineering at Northwestern University in Evanston, Illinois, in 1958.

Appendix 1 – Battery Characteristics

		7.5		10		20		30		40		50		60	
		Low	High	Low	High	Low	High	Low	High	Low	High	Low	High	Low	High
Cell Capacity	Ah	23.72	21.35	31.75	28.60	64.53	58.06	90.00	88.50	90.00	90.00	90.00	90.00	90.00	90.00
Number of Cells		59.00	59.00	59.00	59.00	59.00	59.00	64.00	59.00	87.00	78.00	111.00	99.00	135.00	121.00
Cell Characteristics															
Nominal Voltage	V	3.60	3.60	3.60	3.60	3.60	3.60	3.60	3.60	3.60	3.60	3.60	3.60	3.60	3.60
Mass	kg	0.88	0.80	1.02	0.92	1.57	1.42	1.97	1.94	1.86	1.86	1.79	1.79	1.75	1.75
Disch Power 10 sec 20% SOC	W	1269	1158	1275	1163	1298	1184	1221	1210	923	939	755	758	639	645
Power Density at 10 sec 20% SOC	W/kg	1438	1445	1252	1259	825	832	621	624	497	504	421	422	365	368
Energy	Wh	85	77	114	103	232	209	324	319	324	324	324	324	324	324
Energy Density	Wh/kg	72	71	83	83	109	109	122	122	129	129	134	134	137	137
Power to Energy Ratio	W/Wh	14.86	15.07	11.16	11.30	5.59	5.67	3.77	3.80	2.85	2.90	2.33	2.34	1.97	1.99
Battery Pack Characteristics															
Nominal Voltage	V	212.4	212.4	212.4	212.4	212.4	212.4	230.4	212.4	313.2	280.8	399.6	356.4	486.0	435.6
Mass	kg	65.1	59.1	75.1	68.1	116	105	157.4	142.9	201.8	181.5	248.8	222	295.3	265
Disch Power 10 sec 20% SOC	kW	74.8	68.3	75.2	68.6	76.6	69.9	78.2	71.4	80.3	73.3	83.8	75.0	86.2	78.1
Total Energy	kWh	5.0	4.5	6.7	6.1	13.7	12.3	20.7	18.8	28.2	25.3	36.0	32.1	43.7	39.2